



# Sodium in the Relapsing–Remitting Multiple Sclerosis Spinal Cord: Increased Concentrations and Associations With Microstructural Tissue Anisotropy

Bhavana S. Solanky, PhD,<sup>1\*</sup>  Ferran Prados, PhD,<sup>1,2</sup> Carmen Tur, PhD,<sup>1</sup> Marios C. Yiannakas, PhD,<sup>1</sup> Baris Kanber, PhD,<sup>1,2</sup> Niamh Cawley, PhD,<sup>1</sup> Wallace Brownlee, PhD,<sup>1</sup> Sebastien Ourselin, PhD,<sup>2</sup> Xavier Golay, PhD,<sup>3</sup>  Olga Ciccarelli, PhD,<sup>1</sup> and Claudia A. M. Gandini Wheeler-Kingshott, PhD<sup>1,4,5</sup>

**Background:** Associations between brain total sodium concentration, disability, and disease progression have recently been reported in multiple sclerosis. However, such measures in spinal cord have not been reported.

**Purpose:** To measure total sodium concentration (TSC) alterations in the cervical spinal cord of people with relapsing–remitting multiple sclerosis (RRMS) and a control cohort using sodium MR spectroscopy (MRS).

**Study Type:** Retrospective cohort.

**Subjects:** Nineteen people with RRMS and 21 healthy controls.

**Field Strength/Sequence:** 3 T sodium MRS, diffusion tensor imaging, and 3D gradient echo.

**Assessment:** Quantification of total sodium concentration in the cervical cord using a reference phantom. Measures of spinal cord cross-sectional area, fractional anisotropy, mean diffusivity, radial diffusivity, and axial diffusivity from <sup>1</sup>H MRI. Clinical assessments of 9-Hole Peg Test, 25-Foot Timed walk test, Paced Auditory Serial Addition Test with 3-second intervals, grip strength, vibration sensitivity, and posturography were performed on the RRMS cohort as well as reporting lesions in the C2/3 area.

**Statistical Tests:** Multiple linear regression models were run between sodium and clinical scores, cross-sectional area, and diffusion metrics to establish any correlations.

**Results:** A significant increase in spinal cord total sodium concentration was found in people with RRMS relative to healthy controls ( $57.6 \pm 18$  mmol and  $38.0 \pm 8.6$  mmol, respectively,  $P < 0.001$ ). Increased TSC correlated with reduced fractional anisotropy ( $P = 0.034$ ) and clinically with decreased mediolateral stability assessed with posturography ( $P = 0.045$ ).

**Data Conclusion:** Total sodium concentration in the cervical spinal cord is elevated in RRMS. This alteration is associated with reduced fractional anisotropy, which may be due to changes in tissue microstructure and, hence, in the integrity of spinal cord tissue.

**Level of Evidence:** 1

**Technical Efficacy Stage:** 2

J. MAGN. RESON. IMAGING 2020.

**M**ULTIPLE SCLEROSIS (MS) can affect the whole central nervous system, including the brain, optic nerves, and the spinal cord, and is characterized by neuroinflammation leading to demyelination and neuronal

View this article online at [wileyonlinelibrary.com](http://wileyonlinelibrary.com). DOI: 10.1002/jmri.27201

Received Feb 22, 2020, Accepted for publication May 6, 2020.

\*Address reprint request to: B.S.S., UCL Queen Square Institute of Neurology, National Hospital for Neurology & Neurosurgery Queen Square, London, WC1N 3BG, UK. E-mail: [b.solanky@ucl.ac.uk](mailto:b.solanky@ucl.ac.uk)

Contract grant sponsor: UK MS Society (programme grant number 984); Contract grant sponsor: UCLH charities and the Clinical Research and Development Committee (CRDC); Contract grant sponsor: National Institute for Health Research University College London Hospitals Biomedical Research Centre (BRC).

From the <sup>1</sup>NMR Research Unit, Queen Square MS Centre, UCL Queen Square Institute of Neurology, Faculty of Brain Sciences, University College London, London, UK; <sup>2</sup>Translational Imaging Group, Centre for Medical Image Computing, Department of Medical Physics and Biomedical Engineering, University College London, London, UK; <sup>3</sup>Brain Repair and Rehabilitation, Queen Square Institute of Neurology, University College London, London, UK; <sup>4</sup>Department of Brain and Behavioural Sciences, University of Pavia, Pavia, Italy; and <sup>5</sup>Brain MRI 3T Research Centre, IRCCS Mondino Foundation, Pavia, Italy

This is an open access article under the terms of the Creative Commons Attribution License, which permits use, distribution and reproduction in any medium, provided the original work is properly cited.

damage. The metabolic mechanisms behind the neurodegeneration remain poorly understood. Recently, studies have suggested that the neuronal loss maybe driven by an accumulation of sodium in tissue, resulting from a disturbance in the delicate balance of the  $\text{Na}^+/\text{K}^+$  pump, leading to a toxic increase in intra-axonal  $\text{Ca}^{2+}$ .<sup>1,2</sup>

With the emergence of ultrashort echo-time (TE) sequences, using sodium ( $^{23}\text{Na}$ ) magnetic resonance imaging (MRI) for noninvasive measures of sodium in vivo has become clinically feasible.<sup>3</sup> The quantitative assessment of total sodium concentration (TSC) in healthy and MS subjects has led to new in vivo evidence on the involvement of sodium ion accumulation in MS.<sup>4-8</sup> A TSC increase in the brain has been correlated with disability in relapsing–remitting MS (RRMS) patients.<sup>4,5</sup> However, the mechanisms of TSC changes in the spinal cord and their clinical relevance in MS is unclear.

$^{23}\text{Na}$ -MRI in the spinal cord remains a challenge mainly due to the small cross-sectional area (CSA) of the cord and inherent limitations of sodium imaging, such as low signal-to-noise ratio and ultrashort  $T_2$  relaxation components of the sodium signal (<5 msec).<sup>9</sup>

To overcome these drawbacks, we have proposed an alternative approach using instead  $^{23}\text{Na}$  MR spectroscopy ( $^{23}\text{Na}$ -MRS), which has proven successful in healthy subjects.<sup>10</sup> Using this method, a single large voxel is acquired covering a portion of the cervical spinal cord to maximize the measurable signal.

In this work we measured TSC alterations in the cervical spinal cord of people with RRMS and a control cohort and investigated the associations with cross-sectional area, diffusion metrics, lesion presence, and clinical scores.

## Materials and Methods

All subjects provided written informed consent and the study was approved by the Institutional Research Ethics Committee. Inclusion criteria were no known neurological conditions (except MS for RRMS group), age 18–65, and no contraindications for an MRI study. Also, the ability to comfortably get off the scanner bed with the aid of a step.

### Subjects

Ambulatory patients with RRMS attending MS clinics at the National Hospital for Neurology and Neurosurgery (London, UK) were invited to take part in the study. A total of 19 people with an RRMS diagnosis<sup>11</sup> and 21 healthy controls (HCs) were recruited (mean age [SD]: 46 [10] years, 17 female and 34 [9] years, 9 female, respectively).

Group sizes were determined based on previous work in HC (10) and the reported TSC in RRMS normal-appearing white matter (NAWM) brain tissue (6) (power 0.8,  $P = 0.05$ ), which determined a sample size of  $n = 16$  per group. Groups were larger to manage any potential data rejection.

### MRI

Volunteers underwent MRI on a 3T Achieva TX system (Philips Healthcare, Best, The Netherlands). The Q-Body coil was used to

acquire  $^1\text{H}$   $T_2$ -weighted turbo spin echo (2D  $T_2$ w-TSE) images of the cervical cord in the sagittal and coronal planes to facilitate positioning of the  $^{23}\text{Na}$ -MRS voxel.

A fixed tuned transmit-receive sodium coil (Rapid, Germany) was used for acquiring  $^{23}\text{Na}$ -MRS. Subjects were positioned so the C2/3 level was covered by the sensitive area of the coil. An image-selected in vivo spectroscopy (ISIS) sequence was used to select a voxel ( $9 \times 12 \times 35 \text{ mm}^3$ ), centered on the C2-3 intervertebral disc (Fig. 1).<sup>10</sup> To ensure minimal contamination from cerebrospinal fluid (CSF) and bones, inner-volume saturation pulses (slabs) were positioned in the anterior–posterior and right–left directions. Given that ISIS is susceptible to motion, the sodium exam was kept very short (4 minutes for the sodium MRS), and cardiac triggering was not employed; this meant a shorter relaxation time (TR) (300 msec) was achievable. Additionally, a neck brace was used to eliminate motion during the scan. In all, 800 averages were collected with a sweepwidth of 6000 Hz and 1024 samples. An identical  $^{23}\text{Na}$ -MRS scan was acquired on an external calibration reference phantom containing 44.8 mM NaCl, with similar loading to the human head, for quantification.<sup>10</sup>

### $^{23}\text{Na}$ Quantification

Data were processed using jMRUI<sup>12,13</sup> and underwent phasing, apodization (20 Hz), and zero-filling (2048), using the AMARES algorithm. Differences in  $T_1$  and  $T_2$  values between phantom and tissue were also accounted for, as previously reported, using relaxation rates from healthy brain tissue.<sup>14,15</sup> The ratio of the two corrected signals was then used to quantify the sodium concentration for each volunteer.<sup>10</sup> As phantom loading was similar to a human head, no corrections for loading were performed for either group.

### $^1\text{H}$ MRI

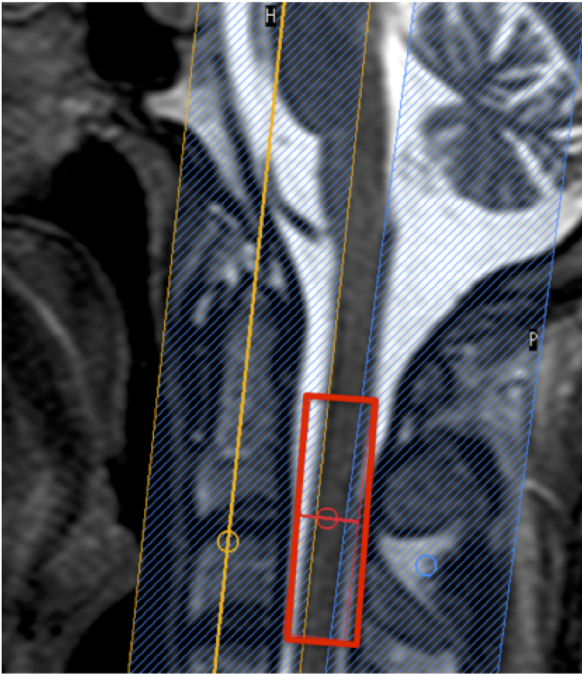
**MEASUREMENT OF CSA.**  $^1\text{H}$  gradient echo images, covering the same area as the MRS voxel, were acquired using a 16-channel neurovascular coil. 3D fat-suppressed fast field-echo (3D-FFE) scans were acquired in the axial plane consisting of 10 contiguous slices ( $0.5 \times 0.5 \text{ mm}^2$  resolution, 5-mm slice thickness, TR / echo time [TE] = 23/5 msec, flip angle =  $7^\circ$ ,  $180 \times 240 \text{ mm}^2$  field of view), scan time 14 minutes.

CSA was computed automatically from the 3D-FFE for each subject using a spinal cord (SC) segmentation algorithm,<sup>16</sup> which uses an external and independent database of spinal cord images and their associated segmentations to extract a spinal cord mask for each slice (Fig. 2). These masks were then used to find the average CSA corresponding to the  $^{23}\text{Na}$ -MRS voxel.

**DTI.** A reduced field-of-view echo-planar (ZOOM-EPI) diffusion tensor imaging (DTI) sequence was acquired, with 30 evenly distributed diffusion gradient directions at  $b = 1000 \text{ s/mm}^2$  and three non-diffusion-weighted ( $b = 0$ ) volumes.<sup>17,18</sup> The DTI was cardiac triggered at 4RR,  $1 \times 1 \text{ mm}^2$  resolution, 5-mm slice thickness, TE = 52 msec, field of view =  $64 \times 48 \times 50 \text{ mm}^3$ , 10 slices, SENSE factor 1.5, and a total scan time of 8 minutes.

Each diffusion-weighted image was corrected for eddy current-induced distortions and subject movements using NiftyReg.<sup>19</sup> The NiftyFit toolbox was used to compute standard DTI metrics,<sup>20</sup>

a



b

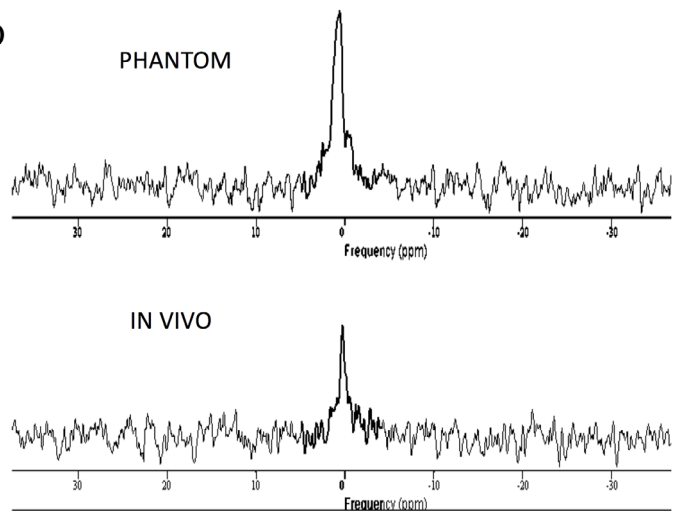


**FIGURE 1: (a)** 2D  $T_2$ -weighted turbo spin-echo (2Dw-TSE) scan in the sagittal plane showing the  $^{23}\text{Na}$  magnetic resonance spectroscopy voxel positioning (red) and the placement of the saturation slabs (dashed blue with orange contour and midline), and **(b)** representative spectra from in vivo and phantom scans.

including fractional anisotropy (FA), radial diffusivity (RD), mean diffusivity (MD), and axial diffusivity (AD).

Using the  $b = 0$  images from the diffusion-weighted scans, masks of the spinal cord were manually drawn in FSLview (<https://fsl.fmrib.ox.ac.uk/fsl/>); the masks were subsequently eroded in-plane by one voxel to reduce partial volume effects between tissue and the surrounding CSF; slices beyond the  $^{23}\text{Na}$ -MRS voxel were excluded from the mask (Fig. 3). These masks were used to extract mean FA, RD, MD, and AD values for each subject.

**LESION COUNT.** Lesion count was considered by noting lesions on the 3D-FFE slices, which covered the  $^{23}\text{Na}$ -MRS voxel by two experienced raters independently (M.Y., 10 years' experience and B.S., 3 years' experience). We recorded 1) if diffuse lesions were present; 2) if focal lesions were present; and 3) any type of lesion was present in addition to the percentage of slices affected by lesions.

### Clinical Assessments

The following assessments were carried out on the RRMS cohort only, on the same day as the MRI examination: Multiple Sclerosis Functional Composite (MSFC), grip strength, vibration sensitivity, and posturography as part of the research. The expanded disability status scale (EDSS) score was gathered from the most recent clinical exam (0–12 months from date of scan).

**MSFC.** RRMS patients were asked to perform the 9-Hole Peg Test (9-HPT),<sup>21,22</sup> 25-Foot Timed walk test (TWT),<sup>23</sup> and Paced Auditory Serial Addition Test with 3-second intervals (PASAT-3).<sup>24</sup> The z scores were calculated for 9-HPT and TWT, and the three tests were used to find the MSFC for each subject using the task force database.<sup>22,23</sup>

**GRIP STRENGTH AND VIBRATION SENSITIVITY.** Mean grip strength from the upper and lower limbs was measured using the

a



b



c

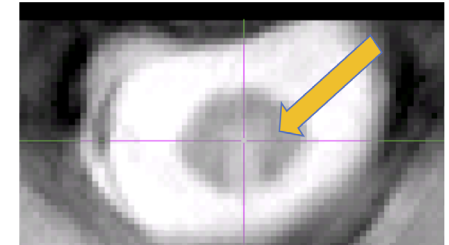


**FIGURE 2:  $^1\text{H}$  MRI of the cervical cord in the axial plane, covering the same volume as the  $^{23}\text{Na}$  MR spectroscopy voxel, showing (a) an example slice through cervical 2/3 level of a healthy control, (b) the binary mask corresponding to the cross-sectional area, and (c) the presence of a lesion (shown in a patient).**

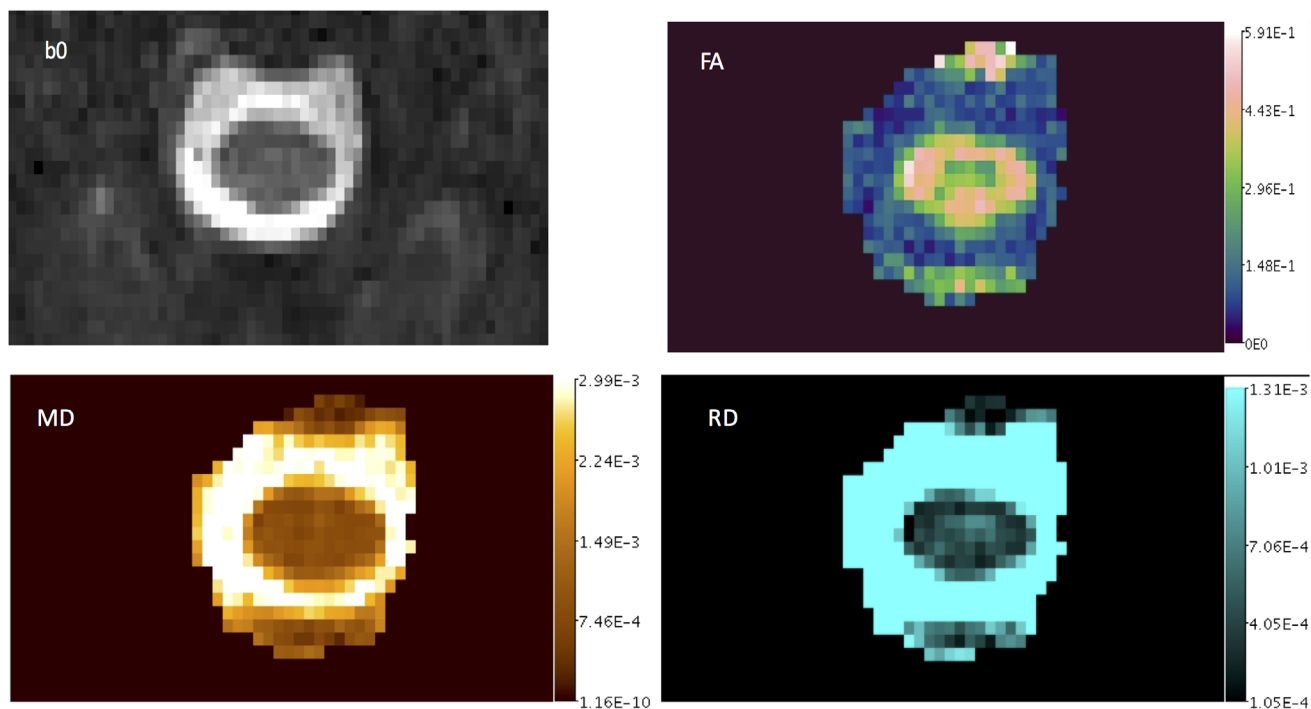


**FIGURE 3:** Reduced field-of-view echo-planar imaging examples of a  $b_0$  image and fractional anisotropy (FA), mean diffusivity (MD), and radial diffusivity (RD) maps

Jamar hydraulic dynamometer (Sammons Preston, Bolingbrook, IL).<sup>25</sup>

Vibration perception thresholds (VPTs) were measured from all four limbs at the lateral malleoli and ulna styloid processes using the biothesiometer (Bio-Medical Instrument, Newbury, OH). Mean VPTs were calculated and used in the analysis.

**POSTUROGRAPHY.** A 3D orientation sensor (MTx: Xsens, Enschede, NL), attached below the shoulder blades, measured the motion in the trunk in the anteroposterior (pitch) and mediolateral (roll) planes and was sampled at 100 Hz.<sup>26</sup> Postural stability was assessed by asking subjects to stand facing a blank wall at a distance of 1 m, for 40-second intervals. Three trials of each of four conditions, consisting of two stance widths (inter-malleolar distance of 32 cm and 4 cm) and two visual conditions (eyes either open or closed), were recorded. The means of the three trials per condition were used for statistical analysis.

### Statistical Analysis

To assess interobserver lesion count agreement between raters, the intraclass correlation coefficient (ICC) was calculated for focal, diffuse, and total lesion percentage.

Multiple linear regression models were built with Stata/SE 14.2 (StataCorp, College Station, TX) used to investigate differences in TSC between RRMS and HC groups. In these models, TSC was considered the dependent variable and cohort (patient/control) was considered an independent variable. These models were adjusted for potential confounders such as age, gender, CSA, and the presence of lesions in the spinal cord. As a secondary analysis, differences in CSA between patients and controls were also assessed through linear regression in a similar way.

Multiple linear regression models were also built to identify associations between TSC and CSA and DTI metrics in RRMS patients. In these models, TSC was considered the dependent variable and CSA or a DTI metric (one at a time) was considered the explanatory variable. Similar models were also built to investigate whether TSC is affected by the presence of lesions by including lesion presence as the main explanatory variable. These models were also adjusted for potential confounders.

Finally, to investigate the relationship between TSC and clinical scores, a new set of multiple linear regression models were built, where the clinical score (one at a time) was considered the dependent variable and TSC an independent variable, together with potential confounders. A significance level of 0.05 was used. As we were testing for multiple null hypotheses, no correction was made for multiple comparisons, as the error for this would be reported with every test.<sup>27,28</sup>

### Results

MSFC scores were found to range between  $-2$  to  $0.9$ . Mean disease duration was 12.8 years, range 1.7–42 years. All patients except two had lesions present in the area covered by the MRS voxel. On average, 23% of the slices covering the voxel contained focal lesions (range 0–90%), and 37% contained diffuse lesions (range 0–80% of slices).

### TSC

Table 1 summarizes the MRI measures for each group. TSC was rejected in five HC and four RRMS participants due to large motion and/or other artifacts. TSC in the cervical cord was significantly higher in the RRMS group relative to HC

even when adjusted for age and gender ( $F_{3,25} = 6.57$ , adjusted  $R^2 = 0.38$  mmol,  $\beta = 10.98$  mmol,  $P = 0.038$  with a 95% confidence interval [CI] of [0.6, 21.3]), and when corrected for CSA, the relationship remained largely unchanged ( $F_{4,24} = 4.78$ , adjusted  $R^2 = 0.35$ , mmol  $\beta = 10.64$  mmol,  $P = 0.053$ ), albeit with a loss in significance. No association was found between CSA and TSC ( $P = 0.082$ ) and this remained the case when corrected for age ( $P = 0.37$ ), gender ( $P = 0.88$ ), and cohort ( $P = 0.727$ ).

### Diffusion Metrics

FA in the RRMS group was significantly reduced relative to HC after adjusting for age and gender, ( $F_{3,35} = 5.52$ , adjusted  $R^2 = 0.26$ ,  $\beta = -0.03$ ,  $P = 0.044$ , and 95% CI [-0.05, -0.0008]). There were no significant differences between groups when comparing AD ( $P = 0.45$ ), MD ( $P = 0.842$ ), or RD ( $P = 0.371$ ) when taking into account age and gender. We also checked if these changed when adjusted for the presence of lesions, which also proved to have no significance ( $P > 0.05$  for all). When CSA was taken into account, FA and AD were significantly different between groups ( $F_{2,35} = 7.06$ , adjusted  $R^2 = 0.2469$ ,  $\beta = -0.04$ ,  $P = 0.005$ , and  $F_{2,34} = 7.19$ , adjusted  $R^2 = 0.2972$ ,  $\beta = -0.00008$ ,  $P = 0.008$ , respectively) and a trend was seen in MD ( $P = 0.07$ ).

We found that increased TSC was also associated with reduced FA ( $F_{1,26} = 5.03$ , adjusted  $R^2 = 0.13$ ,  $\beta = -122$  mmol,  $P = 0.034$ ) (Fig. 4). No associations were found between TSC and MRI markers.

### Lesions

Lesion presence scores were in total agreement between the two raters (lesion percentage ICC > 0.98).

No association was detected between TSC and the percentage of focal or diffuse lesions ( $P = 0.310$  and

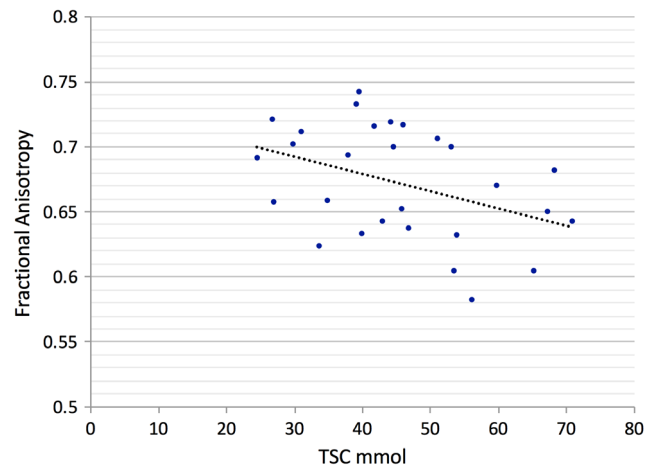


**FIGURE 4: Unadjusted association between increased total sodium concentration (TSC) and reduced fractional anisotropy (FA) ( $F_{1,26} = 5.03$ ,  $R^2 = 0.16$ ,  $\beta = -122$  mmol per unit FA,  $P = 0.034$  for the unadjusted model).**

$P = 0.402$ , respectively). When exploring associations between TSC and the percentage of slices containing any type of lesion ( $P = 0.862$ ), no significant association was found either.

### Clinical Scores and MRI Biomarkers

Posturography reports were acquired on 11 of the 19 scanned patients. A significant association between posturography measures and TSC in the spinal cord was found: higher roll with eyes closed (REC\_4cm) was associated with higher TSC levels in the spinal cord ( $F_{1,9} = 5.78$ , adjusted  $R^2 = 0.3234$ ,  $\beta = 0.006$ ,  $P = 0.040$ , Table 2). This correlation was still present if the presence of lesions was also taken into account, ( $F_{2,8} = 4.28$ , adjusted  $R^2 = 0.3963$ ,  $\beta = 0.007$  mmol<sup>-1</sup>,  $P = 0.025$ ). This association was also reinforced by a trend in the decline of roll with foot stance 4 cm and eyes open ( $P = 0.075$ ). When the presence of diffuse lesions was taken

**TABLE 1. Summary of the Mean Total Sodium Concentration (TSC), Cross-Sectional Area (CSA), Fractional Anisotropy (FA), Radial Diffusivity (RD), Mean Diffusivity (MD), and Axial Diffusivity (AD) in Healthy Controls and People With Relapsing–Remitting Multiple Sclerosis (RRMS)**

	Healthy controls	RRMS	Uncorrected $P$ value	Corrected $P$ value**
TSC (mmol)	38.0 ± 8.6	57.6 ± 18**	<0.001	0.038
CSA mm <sup>2</sup>	82.4 ± 6.4	76.8 ± 8.2*	0.021	0.182
FA	0.69 ± 0.03	0.65 ± 0.04*	0.003	0.044
RD	0.00049 ± 0.00006	0.00050 ± 0.00006	0.663	0.371
MD	0.0010 ± 0.00008	0.0009 ± 0.00005*	0.044	0.842
AD	0.0018 ± 0.00009	0.0017 ± 0.00008*	0.001	0.453

\*Statistically significant.

\*\*Corrected for age and gender.

**TABLE 2. Association Between Increase in Total Sodium Concentration (TSC) and Clinical Scores**

	Regression coefficient	95% CI	<i>P</i> value*	<i>P</i> value**
z 9HPT	0.00022	−0.00050, 0.00095	0.50	0.367
z TWT	.0017	−0.0016, 0.0051	0.28	0.219
PASAT-3	0.32	−0.52, 1.16	0.402	0.228
MSFC	0.02	−0.03, 0.07	0.40	0.207
Grip	0.12	−0.19, 0.42	0.42	0.534
VPT wrist	−0.049	−0.20, 0.10	0.483	0.465
VPT ankle	−0.018	−0.88, 0.53	0.584	0.393
Posturography				
32 cm eyes open				
Roll	0.004	−0.003, 0.011	0.208	0.193
Pitch	0.006	−0.007, 0.017	0.342	0.401
Sway	0.007	−0.007, 0.022	0.282	0.322
4 cm eyes open				
Roll	0.005	−0.0018, 0.012	0.127	0.084
Pitch	0.0017	−0.008, 0.011	0.687	0.564
Sway	0.005	−0.007, 0.017	0.377	0.283
32 cm eyes closed				
Roll	0.003	−0.01, 0.016	0.596	0.541
Pitch	−0.0009	−0.026, 0.024	0.937	0.989
Sway	0.0012	−0.030, 0.032	0.927	0.861
4 cm eyes closed				
Roll	0.0065	−0.0008, 0.0138	0.052	0.045*
Pitch	0.003	−0.005, 0.011	0.382	0.396
Sway	0.007	−0.004, 0.018	0.178	0.178
Lesions			unadjusted	
% with focal	12.319	−13, 37	0.310	
% with diffuse	−11.36	−40, 17	0.402	
Total %	1.52	−17, 20	0.862	

\**P* value when adjusted for age and gender.

\*\**P* adjusted for gender and cross-sectional area (CSA).

into account, both REC\_4 cm and roll with eyes open (REC\_4cm) correlated with sodium concentrations ( $F_{2,8} = 4.08$ , adjusted  $R^2 = 0.3811$ , beta = 0.006 degrees per mmol,  $P = 0.033$ , and  $F_{2,8} = 6.19$ , adjusted  $R^2 = 0.5092$ , beta = 0.005 degrees per mmol increase in sodium,  $P = 0.031$ , respectively) (Table 4).

All 19 subjects successfully underwent measures for MSFC. CSA was associated with MSFC: this was explained

by its association with the inverse of 9-HPT and supported by a significant association with recorded EDSS (Table 3). FA was also found to be significantly correlated with posturography measures REC\_4cm,  $F_{4,10} = 1.79$ , adjusted  $R^2 = 0.1838$ , beta = −1.70 degrees per unit FA,  $P = 0.044$  when corrected for age, gender, and CSA; however, when any lesion presence was also added as a covariant, this became nonsignificant ( $P = 0.075$ ).

**TABLE 3. Associations Between <sup>1</sup>H MRI Measures: Axial Diffusivity (AD), Mean Diffusivity (MD), Fractional Anisotropy (FA), Radial Diffusivity (RD), and % Number of Slices With Focal Lesions (% w Focal Lesions) With Clinical Scores Corrected for Age and Gender**

MRI biomarker	Clinical score	Regression coefficient	95% CI	P value
CSA	EDSS	-0.12	-0.22, -0.02	<0.03
	z-9HPT	0.0007	0.000, 0.001	0.03
	MSFC	0.05	0.001, 0.01	<0.05
FA	Roll eyes closed_4cm	-1.59	-3.17, -0.01	0.048
% w focal lesion	EDSS	4.2	1.3, 7.1	0.009
	z-TWT	-0.11	-0.18, -0.02	0.016
	z-9HPT	-0.02	-0.04, -0.007	0.009
	Average ankle VBT	22	5.6, 38.4	0.012
	PASAT	-26	-48.7, -2.8	0.031
	MSFC	-1.6	-2.84, -0.43	0.012
	Roll eyes closed_4cm	0.28	0.008, 0.548	0.048

The %focal lesion was found to be most sensitive to clinical measures with associations found for MSFC (supported by associations with inverse TWT, inverse 9-HPT, and PASAT-3) as well as VBT in the ankle, and again posturography measures REC\_4cm. When focal lesions were accounted for, it was found that 9HPT, MSFC, and PASAT-3 were all correlated with sodium concentrations (Table 4).

## Discussion

Our exploratory study reports differences in in vivo spinal cord TSC obtained in a cohort of healthy controls and patients with RRMS. TSC in the cervical cord was found to

be statistically significantly higher in RRMS than in HC. We explored possible correlations between TSC increase and a range of structural features and assessed the relevance of TSC for a number of clinical biomarkers.

We found that the increase in TSC is associated with a reduced FA and clinically with poorer mediolateral balance. <sup>23</sup>Na-MRS has shown that a 50% increase in TSC in the cervical spinal cord is present in RRMS patients, independently of CSA, once age and gender have been taken into account. This increase in TSC promises to be a potential sensitive imaging biomarker, given its large effect size. The increased TSC could be associated with two processes involved in the pathology of MS: demyelination and axonal loss, which

**TABLE 4. Significant Associations Between Increase in Total Sodium Concentration (TSC) and Some Clinical Scores, Adjusted for Age, Gender, and Presence of Focal Lesions**

Sodium	Corrected for focal lesions		Corrected for diffuse lesions	
	P value	Beta [95% CI]	P value	Beta [95% CI]
z 9HPT	0.048	0.0007 [0.0001, 0.001]	0.452	
PASAT-3	0.032	0.873 [0.1, 1.6]	0.307	
MSFC	0.022	0.071 [0.01, 0.12]	0.256	
Roll 4 cm eyes open	0.225		0.031	0.005 [0.0006, 0.01]
Roll 4 cm eyes closed	0.089		0.033	0.006 [0.0006, 0.01]

Notably, some clinical tests were also found to be significantly correlated with sodium when corrected for the presence of diffuse lesions; these have also been included. However, significance diminished when age, gender, and CSA were added as covariants.

would increase the extracellular space, which has a much higher sodium concentration (145 mM vs. 10–12 mM intracellular)<sup>29,30</sup> and dysfunction in sodium channels, causing an increase in intracellular sodium.<sup>31</sup> It is, however, difficult to differentiate between both explanations using the current state-of-the-art technology.

We found no association between the increase in TSC and spinal cord CSA, and hence atrophy. This could be taken as meaning, if atrophy is a sign of axonal loss, the increase in TSC in our cohort cannot be explained simply by an increase of extracellular sodium due to axonal death. We should also take into consideration that while RRMS CSA was lower on average than in HC, in contrast to numerous studies, it was not significantly different between the two groups once age and gender were corrected for, possibly due to a limited sample size.<sup>32–35</sup> Our sensitivity to this difference could also be impaired by the low EDSS of our patient cohort (median = 2.5), which was a prerequisite for inclusion in the study due to some of the physical challenges of the MRI protocol at the time. Moreover, there was a disparity in matching age and gender between our groups, which might have affected results despite the applied statistical correction.

Reduced FA was found in the RRMS patients, in agreement with previous studies.<sup>36,37</sup> Reduced FA is seen when pathological processes disrupt the coherence of white matter (WM) fibers. However, our data has shown that while TSC is associated with reduced FA, it is not associated with the presence of lesions; and it has been previously reported that a reduction in FA in the normal-appearing spinal cord tissue is consistent with nonlesional diffuse damage in the cord.<sup>36</sup>

No associations were seen with RD, which has been proposed as a marker for demyelination,<sup>38</sup> nor with MD, which increases in the presence of lesions and inflammation.<sup>39</sup> Together this suggests that the increase in TSC is not due only to an increase in extracellular space and supports the hypothesis that an increased intracellular sodium concentration may also contribute to the elevated TSC. This is further corroborated by the fact that no associations were seen between an increase in TSC in patients and the percentage of slices including focal, diffuse, and any kind of (total) lesions, which would have supported a role of inflammation and tissue disruption on the results. This is not surprising, though, given the narrow distribution of the clinical scores reflecting the mild MS severity of this cohort.

Interestingly, increased TSC was also found to be associated with a poorer mediolateral balance at 4 cm (REC\_4 cm and REO\_4cm) when the presence of *diffuse* lesions was accounted for. While other posturography rates were not found to be significantly associated with increased TSC, regression coefficients showed a trend between increased TSC and poorer balance across the posturography measures. Accounting only for focal lesions did not provide a

significant correlation. Diffuse lesions had a larger impact on posturography scores, perhaps due to the fact that they affected more of the spinal cord. 9HPT, MSFC, and PASAT-3 were found to be significantly correlated with sodium when *focal* lesions were accounted for. Focal lesions at C2/3 are likely to affect 9HPT and MSFC, as both involve the upper limb motion. However, the correlation to PASAT-3 was surprising, given that it is commonly used to test cognitive function.<sup>40</sup> This could be related to an overall increase in sodium in the CNS or the fact that a focal lesion in the spinal cord may be indicative of lesions in cognitive areas of the brain too. Interestingly, for these tests and REO\_4 cm the significance diminished if corrected for the presence of *any* lesion.

Our results suggest the sensitivity of TSC to pathological changes may also be useful for studying other types of MS. For example, it has been reported that metabolic changes (glutamate-glutamine [Glx] and N-acetyl-aspartate [tNAA]) in the same area of the spinal cord of people with primary progressive MS (PPMS,  $n = 21$ ) were associated with an increase in postural sway.<sup>26</sup> Sodium accumulation could trigger the release of excess glutamate, leading to lethal neuroexcitotoxicity, which could in turn lead to decreases in tNAA. Additionally, increased q-space imaging-derived perpendicular diffusivity of the cervical spine was reported to be associated with increased sway in the same PPMS study.<sup>26</sup> This result is similar to what we have found in the present RRMS cohort using DTI metrics, where there was an association between FA and roll at 4 cm.

Our results show TSC in the spinal cord is similar to values measured in the cortical gray matter (GM) (36 mmol) for HCs.<sup>6</sup> However, the spinal cord TSC value in RRMS patients are much higher than both NAWM (34 mmol) and lesions in the brain (42.1 mmol).<sup>6</sup> This could be explained in part by the large MRS voxel, which includes varying fractions of WM, GM, lesion, and central canal fluid. Images with adequate resolution to perform segmentation were not feasible to acquire in the scan session; hence, such tissue fractions were not accounted for in our model.

In contrast to the prior study,<sup>10</sup> here we chose to omit cardiac triggering, as this reduced the scan time from 13 minutes to 4 minutes, giving a more feasible overall scan time. In addition to this difference in restraint were also used whereby the prior study used polystyrene sphere filled vacuum bag, which may have allowed more subject movement. The shimming routines were also changed from FASTERMAP in the previous study to an iterative shim in the current one, as this was found to be more robust due to failure of the shim convergence in the FASTERMAP routine on a number of the subjects. It is also worth noting that the previous study had a more moderate sample number of just six subjects, but the values in this study and the previous do overlap for the healthy cohort.<sup>10</sup>



## Limitations

In this study, 19 ambulatory patients with RRMS attending the MS clinics were recruited to test the sensitivity of sodium MRS to changes in sodium concentration in the cervical spinal cord. Ambulatory patients were able to get on and off the MRI bed easily, to enable a straightforward change of coil and to test tolerability; this resulted in a low EDSS and physical disability range over the cohort, and may not fully represent the full spectrum of RRMS patients. The EDSS score used in the analysis was also taken from patient records; future studies could benefit from a measure taken on the day of the scan, which would have been more accurate.

Based on our data, we calculated a sample size of 39 subjects to detect a 20% change in sodium (power 0.8,  $P = 0.05$ ). Given the detected sensitivity to changes, future work should include all MS phenotypes, ie, patients with clinically isolated syndrome and/or secondary progressive MS, recruited according to the latest diagnostic criteria.<sup>11</sup> The larger sample size calculated with respect to our initial estimate is due largely to a greater standard deviation of sodium concentration in RRMS than in the control group, a variation that was not available to us before this study. Our small sample number may have reduced the power of this study to detect weak correlations, and thus the results should be interpreted with caution.

The presence of lesions could affect both sodium concentration in the spinal cord and FA. While our measure of lesion presence shows that this is not correlated with the changes in TSC and FA, in future studies one should also acquire a dedicated scan for lesion delineation and lesion volume assessment for a better estimate of the effect of lesions.

Here we corrected the signal from  $T_1$  and  $T_2$  of sodium from healthy brain because values for the spinal cord have not been reported. However, the short TR and TE used should minimize any impact if these change in spinal cord tissue or changes resulting from pathology.

Additionally, a phantom designed to have similar loading to the head and neck was used for quantification. Scans to measure and correct for the loading factor per subject would yield more accurate concentrations; however, given the low EDSS of our patient cohort, this would affect the control and RRMS group equally and, therefore, is unlikely to affect our findings. Future studies of more progressive patients with higher lesion loads may require added corrections for the loading factor.

To the best of our knowledge, there is no gold standard for the measurement of sodium in the spinal cord in healthy subjects, nor in disease to validate our findings and values could only be discussed against brain results.

## Conclusion

TSC in the spinal cord was measured to be increased in RRMS subjects relative to controls and associated with

reduced FA and poorer posturography scores. TSC in the spinal cord was also found to be higher than previously reported in NAWM in the brain for RRMS. Longitudinal studies with larger cohorts and high-resolution scans for tissue-specific segmentation are needed to fully understand the origin of elevated TSC, in addition to its effect on disease progression and disability.

## REFERENCES

1. Waxman SG. Conduction in myelinated, unmyelinated, and demyelinated fibers. *Arch Neurol* 1977;34:585-589.
2. Waxman SG. Axonal conduction and injury in multiple sclerosis: The role of sodium channels. *Nat Rev Neurosci* 2006;7:932-941.
3. Nielles-Vallespin S, Weber MA, Bock M, et al. 3D radial projection technique with ultrashort echo times for sodium MRI: Clinical applications in human brain and skeletal muscle. *Magn Reson Med* 2007;57:74-81.
4. Zaaaroui W, Konstandin S, Audoin B, et al. Distribution of brain sodium accumulation correlates with disability in multiple sclerosis: A cross-sectional Na-23 MR imaging study. *Radiology* 2012;264:859-867.
5. Inglese M, Madelin G, Oesingmann N, et al. Brain tissue sodium concentration in multiple sclerosis: A sodium imaging study at 3 Tesla. *Brain* 2010;133:847-857.
6. Paling D, Solanky BS, Riemer F, et al. Sodium accumulation is associated with disability and a progressive course in multiple sclerosis. *Brain* 2013;136:2305-2317.
7. Petracca M, Fleysler L, Oesingmann N, Inglese M. Sodium MRI of multiple sclerosis. *NMR Biomed* 2016;29:153-161.
8. Petracca M, Vancea RO, Fleysler L, Jonkman LE, Oesingmann N, Inglese M. Brain intra- and extracellular sodium concentration in multiple sclerosis: A 7 T MRI study. *Brain* 2016;139:795-806.
9. Riemer F, Solanky BS, Wheeler-Kingshott CAM, Golay X. Bi-exponential (23) Na T2\* component analysis in the human brain. *NMR Biomed* 2018;31:e3899.
10. Solanky BS, Riemer F, Golay X, Wheeler-Kingshott CAM. Sodium quantification in the spinal cord at 3T. *Magn Reson Med* 2013;69:1201-1208.
11. Kurtzke JF. Rating neurologic impairment in multiple sclerosis: An expanded disability status scale (EDSS). *Neurology* 1983;33(11):1444-1452.
12. Naressi A, Couturier C, Devos JM, et al. Java-based graphical user interface for the MRUI quantitation package. *Magma* 2001;12:141-152.
13. Naressi A, Couturier C, Castang I, de Beer R, Graveron-Demilly D. Java-based graphical user interface for MRUI, a software package for quantitation of in vivo/medical magnetic resonance spectroscopy signals. *Comput Biol Med* 2001;31:269-286.
14. Solanky, B.S., Riemer F, Wheeler-Kingshott CAM, Evaluation of cerebrospinal fluid suppression techniques in sodium MRI at 3T. In: Proc 20th Annual Meeting ISMRM, Melbourne; 2012, 1702.
15. Riemer, F., Solanky B, Clemence M, Bi-exponential 23Na T2\* components analysis in the human brain. In: Proc 20th Annual Meeting ISMRM, Melbourne; 2012.
16. Prados F, Cardoso M.J., Yiannakas M.C. Fully automated grey and white matter spinal cord segmentation. *Sci Rep* 6, 36151 2016. <https://doi.org/10.1038/srep36151>.
17. Naismith RT, Xu J, Klawiter EC, et al. Spinal cord tract diffusion tensor imaging reveals disability substrate in demyelinating disease. *Neurology* 2013;80:2201-2209.
18. Kearney H, Schneider T, Yiannakas MC, et al. Spinal cord grey matter abnormalities are associated with secondary progression and physical disability in multiple sclerosis. *J Neurol Neurosurg Psychiatry* 2015;86:608-614.

19. Modat M, Ridgway GR, Taylor ZA, et al. Fast free-form deformation using graphics processing units. *Comput Methods Programs Biomed* 2010;98:278-284.
20. Melbourne A, Toussaint N, Owen D, et al. NiftyFit: A software package for multi-parametric model-fitting of 4D magnetic resonance imaging data. *Neuroinformatics* 2016;14:319-337.
21. Goodkin DE, Hertsgaard D, Seminary J. Upper extremity function in multiple sclerosis: Improving assessment sensitivity with box-and-block and nine-hole peg tests. *Arch Phys Med Rehabil* 1988;69:850-854.
22. Fischer JS, Rudick RA, Cutter GR, Reingold SC, National MS Society Clinical Outcomes Assessment Task Force. The multiple sclerosis functional composite measure (MSFC): An integrated approach to MS clinical outcome assessment. National MS Society Clinical Outcomes Assessment Task Force. *Mult Scler* 1999;5:244-250.
23. Cutter GR, Baier M.L., Rudick R.A. Development of a multiple sclerosis functional composite as a clinical trial outcome measure. *Brain* 1999; 122:871-882.
24. Rao SM, St Aubin-Faubert P, Leo GJ. Information processing speed in patients with multiple sclerosis. *J Clin Exp Neuropsychol* 1989;11: 471-477.
25. Svens B, Lee H. Intra- and inter-instrument reliability of grip-strength measurements: GripTrack™ and Jamar® hand dynamometers. *Hand Therapy* 2005;10:47-55.
26. Abdel-Aziz K, Schneider T, Solanky BS, et al. Evidence for early neurodegeneration in the cervical cord of patients with primary progressive multiple sclerosis. *Brain* 2015;138:1568-1582.
27. Perneger TV. What's wrong with Bonferroni adjustments. *BMJ* 1998; 316:1236-1238.
28. Rothman KJ. No adjustments are needed for multiple comparisons. *Epidemiology* 1990;1:43-46.
29. Turski PA, Perman WH, Hald JK, Houston LW, Strother CM, Sackett JF. Clinical and experimental vasogenic edema: in vivo sodium MR imaging work in progress. *Radiology* 1986;160:821-825.
30. Perier O, Gregoire A. Electron microscopic features of multiple sclerosis lesions. *Brain* 1965;88:937-952.
31. Trapp BD, Stys PK. Virtual hypoxia and chronic necrosis of demyelinated axons in multiple sclerosis. *Lancet Neurol* 2009;8: 280-291.
32. Losseff NA, Webb S.L., O'Riordan J.I. Spinal cord atrophy and disability in multiple sclerosis: A new reproducible and sensitive MRI method with potential to monitor disease progression. *Brain* 1996;119:701-708.
33. Rashid W, Davies GR, Chard DT, et al. Upper cervical cord area in early relapsing-remitting multiple sclerosis: Cross-sectional study of factors influencing cord size. *J Magn Reson Imaging* 2006;23:473-476.
34. Rashid W, Davies GR, Chard DT, et al. Increasing cord atrophy in early relapsing-remitting multiple sclerosis: A 3 year study. *J Neurol Neurosurg Psychiatry* 2006;77:51-55.
35. Stevenson VL, Leary SM, Losseff NA, et al. Spinal cord atrophy and disability in MS: A longitudinal study. *Neurology* 1998;51:234-238.
36. Hesselstine SM, Law M, Babb J, et al. Diffusion tensor imaging in multiple sclerosis: Assessment of regional differences in the axial plane within normal-appearing cervical spinal cord. *AJNR Am J Neuroradiol* 2006;27:1189-1193.
37. Valsasina P, Rocca MA, Agosta F, et al. Mean diffusivity and fractional anisotropy histogram analysis of the cervical cord in MS patients. *Neuroimage* 2005;26:822-828.
38. Song SK, Yoshino J, Le TQ, et al. Demyelination increases radial diffusivity in corpus callosum of mouse brain. *Neuroimage* 2005;26: 132-140.
39. Werring DJ, Clark CA, Barker GJ, Thompson AJ, Miller DH. Diffusion tensor imaging of lesions and normal-appearing white matter in multiple sclerosis. *Neurology* 1999;52:1626-1632.
40. Tombaugh TN. A comprehensive review of the paced auditory serial addition test (PASAT). *Arch Clin Neuropsychol* 2006;21:53-76.